

# Size-Controllable Synthesis of Monodispersed SnO<sub>2</sub> Nanoparticles and Application in Electrocatalysts

Luhua Jiang,<sup>†</sup> Gongquan Sun,<sup>†</sup> Zhenhua Zhou,<sup>‡</sup> Shiguo Sun,<sup>†</sup> Qi Wang,<sup>†</sup> Shiyou Yan,<sup>†</sup> Huanqiao Li,<sup>†</sup> Juan Tian,<sup>†</sup> Junsong Guo,<sup>†</sup> Bing Zhou,<sup>†,‡</sup> and Qin Xin<sup>\*,†,§</sup>

Direct Alcohol Fuel Cell Laboratory and State Key Laboratory of Catalysis, Dalian Institute of Chemical Physics, P.O. Box 110, Dalian 116023, China, Graduate School of the Chinese Academy of Sciences, Beijing 100039, CAS, China, and Headwaters Nanokinetix, 1501 New York Avenue, Lawrenceville, New Jersey 08648

Received: January 19, 2005; In Final Form: March 3, 2005

Size-controllable tin oxide nanoparticles are prepared by heating ethylene glycol solutions containing SnCl<sub>2</sub> at atmospheric pressure. The particles were characterized by means of transmission electron microscopic (TEM), X-ray diffraction (XRD) studies. TEM micrographs show that the obtained material are spherical nanoparticles, the size and size distribution of which depends on the initial experimental conditions of pH value, reaction time, water concentration, and tin precursor concentration. The XRD pattern result shows that the obtained powder is SnO<sub>2</sub> with tetragonal crystalline structure. On the basis of UV/vis and FTIR characterization, the formation mechanism of SnO<sub>2</sub> nanoparticles is deduced. Moreover, the SnO<sub>2</sub> nanoparticles were employed to synthesize carbon-supported PtSnO<sub>2</sub> catalyst, and it exhibits surprisingly high promoting catalytic activity for ethanol electrooxidation.

## 1. Introduction

Because of its unique electrical and catalytic properties, tin oxide has been widely used for various electrochemical and catalytic applications, such as gas sensors for environmental monitoring<sup>1</sup> and catalysts.<sup>2</sup> For these applications, SnO<sub>2</sub> small particle size or large specific surface area is essential to high performance. Among various chemical synthesis methods for preparation of metal oxides of large surface area, a sol–gel process offers several advantages over other methods, including simple procedure, lower processing temperature, and better homogeneity.<sup>3</sup> Different precursors may be used as starting materials to prepare tin oxides using a sol–gel process such as tin alkoxide<sup>4</sup> and various tin salts.<sup>5</sup> However, tin alkoxides are not only expensive but also extremely sensitive to moisture, heat, and light, implying that the process is difficult to control and not economical. To prepare powders with large specific surface areas, an alcoholic solvent is preferred to water because of its lower surface tension so that a “loose” powder can be obtained from collapsing of gel structure.<sup>6</sup> In addition, another advantage of the process using alcoholic solvent is that the sol solution is stable in the presence of Cl<sup>−</sup>. Since Yamamoto and Sasamoto<sup>7</sup> prepared indium tin oxide thin films using thermal decomposition of indium and tin salts in ethylene glycol solution, researchers have prepared successfully tin oxide particles with different shapes, such as nanowires, nanobelts, and nanoribbons, etc.<sup>8</sup> One prominent feature of these processes is employing complexing reagents to obtain the desired shapes. To improve the stability and purity of these materials, subse-

quent thermal treatments are required. However, thermal treatments lead to an increase of the average grain size, spreading of the grain size distribution, and changes in the phase composition with increasing annealing temperature.

Especially, it is a challenging task to synthesize SnO<sub>2</sub> with controlled particle size. Herein, we describe a simple approach to synthesize uniform tin oxide spherical nanoparticles with controllable size based on ethylene glycol and tin(II) halide. The advantage of this process is no need of protective reagents and thermal treatments. In addition, these nanoparticles in the prepared PtSnO<sub>2</sub>/C catalysts showed a potential high promoting catalytic activity for ethanol electrooxidation.

## 2. Experimental Section

Dihydrate tin(II) halide, ethylene glycol (EG), and sodium hydroxide (A.R.) were used as supplied without further purification. In a typical procedure, 0.2 g of SnCl<sub>2</sub>·2H<sub>2</sub>O (dissolved in 10 mL of EG) was added to 40 mL of EG or a mixture of EG and water that was hosted in a round-bottom flask. If needed, NaOH was added to modify the pH value of the solution. After the solution had been refluxed at 190 °C for a certain time with constant stirring under atmospheric pressure, the clear solution turned into a slight blue or slight yellow colloid with the reaction time increasing. When the reaction conditions were modified, yellow precipitates could be obtained, and after they were filtrated, washed with deionized water, and dried, yellow powder can be obtained.

In a typical procedure, 6 mL of SnO<sub>2</sub> colloid (2 mg mL<sup>−1</sup> Sn) and 162 mg of chloroplatinic acid (Pt content, 37 wt %; dissolved in 8 mL of EG) were added simultaneously to 16 mL of EG that was hosted in a round-bottom flask, following constant stirring for a half-hour. The mixture was maintained at 403 K for 2 h to ensure the complete reduction of Pt. A flow of argon was passed through the reaction system to remove

\* Corresponding author. Fax and telephone: +86-411-84379071. E-mail: xinqin@dicp.ac.cn.

<sup>†</sup> Direct Alcohol Fuel Cell Laboratory, Graduate School of the Chinese Academy of Sciences.

<sup>‡</sup> Headwaters Nanokinetix.

<sup>§</sup> State Key Laboratory of Catalysis, Dalian Institute of Chemical Physics, Graduate School of the Chinese Academy of Sciences.



**Figure 1.** TEM images of nanoparticles prepared at different water content with  $[H_2O]/[EG] =$  (A) 0.01, (B) 0.04, and (C) 0.5 (the scale bar is 20 nm).

oxygen and organic byproducts. When the system was cooled to room temperature, 330 mg of active carbon (Vulcan XC-72, dissolved in 10 mL of EG) was added to the mixed solution. After another half-hour of stirring, the resulting dark-brown mixture was filtered, washed with copious distilled water, and dried at 343 K under vacuum. The obtained electrocatalyst was denoted as  $PtSnO_2/C$ .

The X-ray diffraction (XRD) pattern of the yellow powder was recorded with a Rigaku Rotaflex (RU-200B) X-ray diffractometer using  $Cu\ K\alpha$  radiation with a Ni filter. The tube current was 100 mA with a tube voltage of 40 kV. The  $2\theta$  angular regions between 15 and  $85^\circ$  were explored at a scan rate of  $5^\circ\ min^{-1}$ . Transmission electron microscopy (TEM) investigations of the as-prepared colloid were carried out using a JEOL JEM-2000EX microscope operating at 100 kV. UV–visible spectrophotometry was applied to trace the reaction on a JASCO Model V-550 recording spectrophotometer. To clarify the reaction mechanism, FTIR spectra of EG solution containing  $SnCl_2$  before and after reaction were collected on a Nicolet Avatar-370 equipped with a DTGS detector. A spectrum, collected as the average of 64 scans with a resolution of  $4\ cm^{-1}$ , was recorded from 4000 to  $400\ cm^{-1}$  for the transmission mode.

### 3. Results and Discussion

The dependence of the mean size and the size distribution of the nanoparticles on the experimental conditions—temperature, reaction time, and water content—was investigated both in order to optimize the synthesis and to gain a better understanding of the tin oxide formation.

**3.1. Effect of Water Content.** First of all, the water content of the solvent was found to be a critical parameter. The mean particle size and the size distribution are strongly dependent on the initial molar ratio  $[H_2O]/[EG]$ . In a rigorously dried EG solvent, the mixture solution remains clear and no nanoparticles are observed in the solution even refluxed at  $190^\circ C$  for several hours. We found that the formation of nanoparticles requires the presence of an initial water content in the solution. At the ratio of  $[H_2O]/[EG] = 0.01$ , the color of the mixture changed from transparent to slight blue after being refluxed at  $190^\circ C$  for 40 min. The slight blue color of the colloid may be due to the very small particles in the colloid. It is believed that the particles reflect different colors when the particle sizes decrease to nanometer scale. The TEM image of the above-mentioned colloid shown in Figure 1A also confirms that the particle size is very small. It can be seen clearly that the particle size in the colloid is about 1 nm with sharp distribution. When the water content increased to  $[H_2O]/[EG] = 0.04$ , the color of the colloid

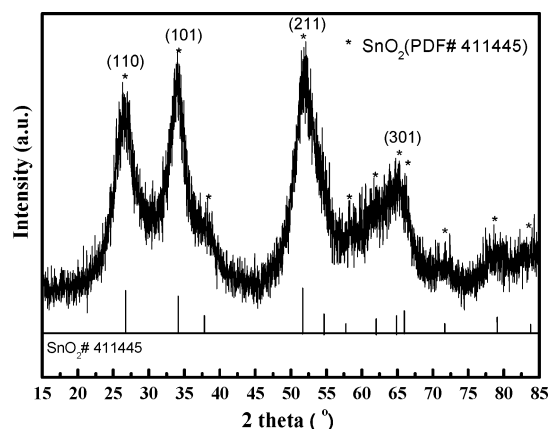


**Figure 2.** XRD pattern of  $SnO_2$  nanoparticles in Figure 1C.

remained light blue after being refluxed at  $190^\circ C$  for 40 min. The TEM image of the colloid is shown in Figure 1B. It can be seen that the nanoparticles' size (Figure 1B) slightly increased. For higher  $[H_2O]/[EG]$  ratios, the color of the solution changed to slight yellow after being refluxed at  $150^\circ C$  for only several minutes, and with time increasing slight yellow precipitates appeared in the solution. Figure 1C is the TEM image of the yellow precipitates prepared with a solvent of  $[H_2O]/[EG]$  (v/v) = 0.5. As can be seen from this figure, the particles agglomerate seriously. Though the primary particle size is only 1–2 nm, they agglomerate to larger particles with a mean size near 10 nm and further collide with each other to form conglomeration. The experimental results indicate that the particle size is sensitive to the water content. The control of the  $SnO_2$  particle size can be realized simply by varying the water content in the reaction system.

To clarify the crystalline structure, an XRD pattern of the as-prepared powder (Figure 1C) is collected and shown in Figure 2. The diffraction peaks at around  $27^\circ$ ,  $34^\circ$ ,  $52^\circ$ , and  $66^\circ$  are assigned to  $SnO_2$  (110), (101), (211), and (301) (PDF No. 411445), respectively. No diffraction peaks due to metallic Sn or other tin oxides were discerned. The diffraction peaks in the XRD pattern broadened due to the particles in the sample are too small. The primary particle size calculated by Sherrer formula is about 1.8 nm. As mentioned above, the primary particle size observed in the TEM image is also less than 2 nm (Figure 1C). Both results agree well with each other.

**3.2. Effect of the pH Value.** In the following experiments,  $SnO_2$  nanoparticles were synthesized at a fixed  $[H_2O]/[EG]$  ratio of 0.01 and a Sn ion concentration of 8 m mol. After being refluxed at  $190^\circ C$  for 6 h, the obtained colloid at different pH

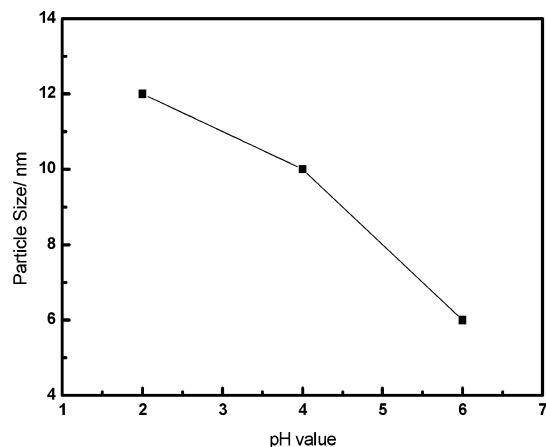


**Figure 3.** SnO<sub>2</sub> particle size vs pH.

values was observed under TEM. The relationship of pH value and the particle size is shown in Figure 3. It can be seen that the particle size is decreased with increasing pH value. Thus, the particle size could be controlled from about 6 to 12 nm by modifying the pH value of the precursor solution from 2 to 6. When the pH value of the solution was above 7, that is, in basic conditions, no particles formed in the solution after being refluxed at 190 °C for 6 h.

**3.3. Effect of Reaction Time.** At a fixed water content and pH value, the mean particle diameter was found to depend on the reaction time. In the following experiments, the water content in the reaction system was fixed at  $[H_2O]/[EG] = 0.01$  and the Sn ion concentration was fixed at 8 m mol and the pH value of the system was controlled at 2. The dependence of particle size on the reaction time was studied in detail. It was observed that the color of the mixture containing SnCl<sub>2</sub> changed to slight blue and transparent after being refluxed for 40 min at 190 °C. A little of such a colloid was extracted and cooled suddenly in an ice–water bath to stop the reaction. The rest of the colloid was refluxed continuously at 190 °C. After another 20 min, the colloid remained slight blue and a little of the colloid was extracted and cooled in an ice–water bath. Continuously refluxing for another 300 min, the transparent slight blue colloid changed gradually to light yellow and a little of the yellow precipitates was observed at the bottom of the flask. A small amount of the yellow colloid was extracted and treated according to the above procedure. The three extracted colloid samples were observed under TEM, and the corresponding images are shown in Figure 4. It can be seen clearly that the particle size increased with the reaction time. When the reaction proceeded in 40 min, the slight blue colloid indicated a very small particle size of

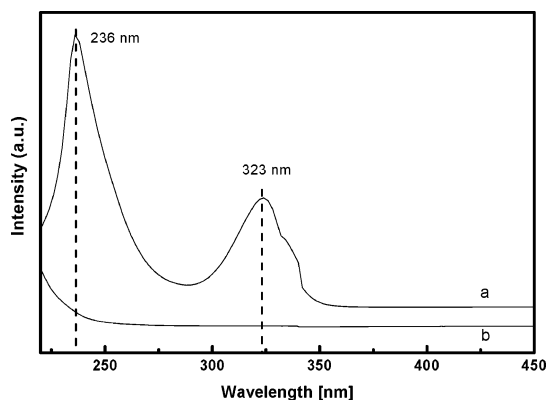


**Figure 5.** UV/vis spectra of (a) SnCl<sub>2</sub> in EG (b) SnO<sub>2</sub> colloid in EG solution.

about 1.2 nm. With the reaction time increasing, the particles grew up gradually, and finally, the slight yellow colloid implied the larger particles of a mean diameter of 12 nm formed.

**3.4. Deduced Particle Formation Mechanism.** UV/vis spectroscopy was used to characterize the reaction process. Figure 5 shows the UV/vis spectra of the precursor SnCl<sub>2</sub> in EG solution ( $[H_2O]/[EG] = 0.01$ ) and the as-obtained colloid after being refluxed at 190 °C for 1 h. The precursor SnCl<sub>2</sub> displays two bands around 236 and 323 nm. However, after the mixture of SnCl<sub>2</sub> and EG was refluxed at 190 °C for 1 h, the two bands disappeared, indicating the change of tin valence. To clarify the valence variation of tin, the UV/vis spectra of SnCl<sub>4</sub> in EG solution was also collected and no band was found in the studied wavelength. Thus, it is deduced that the disappearance of the two bands assigned to bivalent Sn implies formation of tetravalent Sn in EG solution. Combined with the foregoing XRD result, it is confirmed that SnO<sub>2</sub> nanoparticles formed in the EG solution.

To clarify the role EG molecules played in the reaction, FTIR spectra of the reaction system before and after the reaction were studied and are shown in Figure 6. Even though no change was observed in the two spectra, it is impossible to exclude the EG molecules taking part in the reaction for the EG molecules are the overwhelming majority as compared to water. Water is indispensable in the reaction, and water content in the reaction system is decisive for the particle size. The TEM image of the sample (Figure 1C) displays that the particles agglomerate seriously when the water content is increased to some extent. On the basis of the above experimental results, the formation mechanism of SnO<sub>2</sub> particles in EG is deduced (Figure 7). In EG-rich solution, SnCl<sub>2</sub> was surrounded and protected by EG molecules and Cl<sup>−</sup> was replaced by EG molecules.<sup>3</sup> When the

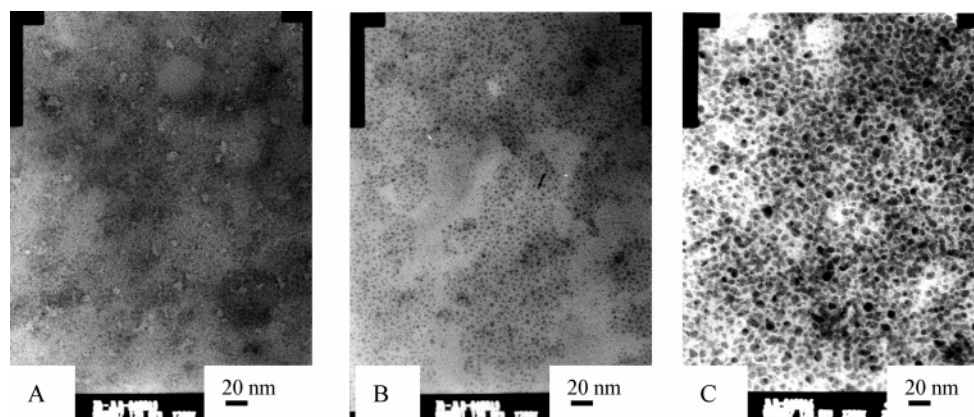


**Figure 4.** TEM images of SnO<sub>2</sub> synthesized in EG solution of various reaction times of (A) 40, (B) 60, and (C) 360 min (the scale bar is 20 nm).



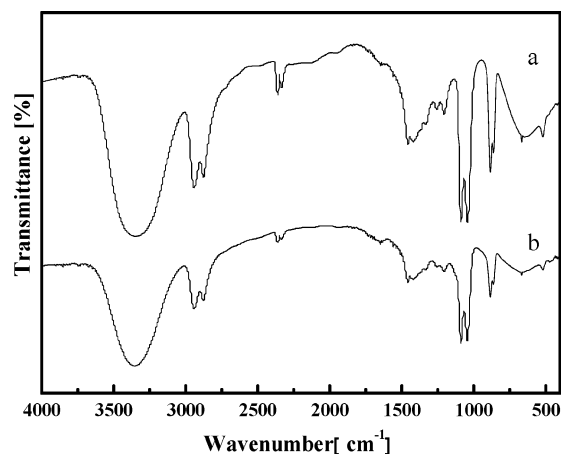


**Figure 6.** FTIR spectra taken from the mixed solutions (a) before and (b) after reaction. The spectra were collected employing a KRS5 window.

system was refluxed in air, the water molecules might attack the  $\text{Sn}-\text{OCH}_2\text{CH}_2\text{OH}$  bonds as a result of replacing the EG molecules to form  $\text{Sn}(\text{OH})_2$  and finally decompose into  $\text{SnO}$  and then was further oxidized by oxygen in air into  $\text{SnO}_2$ .

**3.5. Performance of  $\text{SnO}_2$  Nanoparticles as Anode Catalyst Promoter of Direct Ethanol Fuel Cell.** As an active promoter for Pt catalysts, tin or tin oxide has been added to the Pt/C via electrochemical/chemical deposition to enhance the catalytic activity for alcohol electrooxidation in fuel cells.<sup>2</sup> Especially, compared with the Pt/C catalyst, PtSn/C displayed a much better performance than Pt/C for ethanol electrooxidation. Using the prepared  $\text{SnO}_2$  nanoparticles herein (sample in Figure 1B), PtSnO<sub>2</sub>/C electrocatalyst was prepared. The TEM

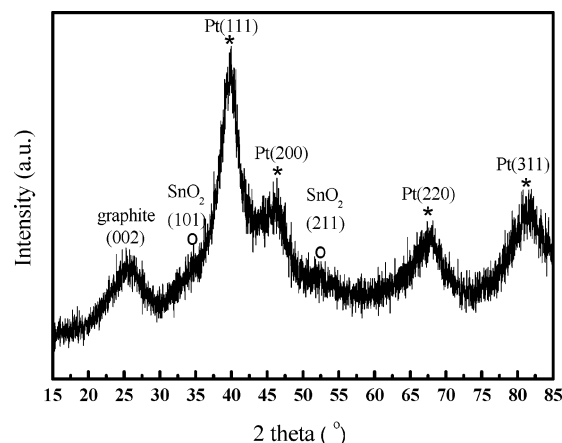


**Figure 9.** XRD pattern of the prepared PtSnO<sub>2</sub>/C electrocatalyst.

image of PtSnO<sub>2</sub>/C is shown in Figure 8. From Figure 8a it can be seen that the metal particles are uniform with sharp distribution. The mean particle size is about 3 nm. The XRD pattern of the PtSnO<sub>2</sub>/C sample (Figure 9) shows the coexistence of  $\text{SnO}_2$  (tetragonal) and Pt (fcc) crystalline. Figure 10 is the performance of ethanol fuel cells with commercial Pt/C (purchased from Johnson Matthey Inc.) and PtSnO<sub>2</sub>/C as the anode catalyst, respectively. From this figure, it can be seen that the maximum power density with Pt/C as anode is only  $10 \text{ mW cm}^{-2}$ , while with PtSnO<sub>2</sub>/C the power density can be up to near  $80 \text{ mW cm}^{-2}$ . PtSnO<sub>2</sub>/C prepared by this method seems to be an excellent catalyst for ethanol electrooxidation. The promoting effect of the tin oxide on the performance of Pt/C catalyst is being studied.

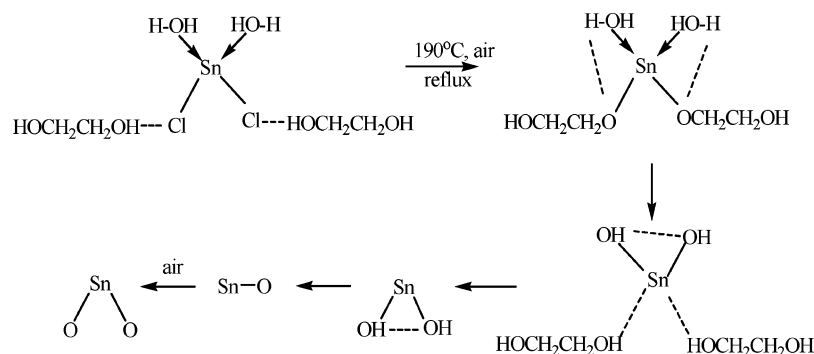


**Figure 7.** Schematic illustration of a proposed mechanism responsible for the formation of  $\text{SnO}_2$  nanoparticles in EG solution.

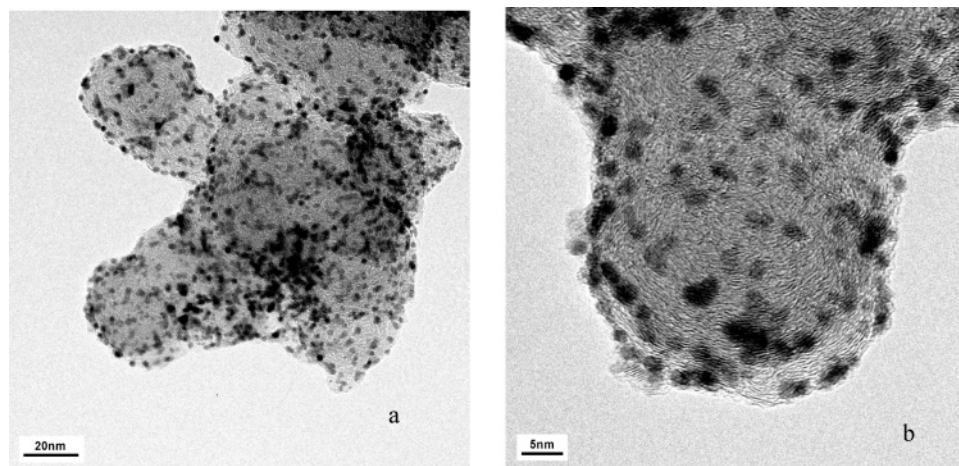


**Figure 8.** (a) TEM and (b) HRTEM images of PtSnO<sub>2</sub>/C.

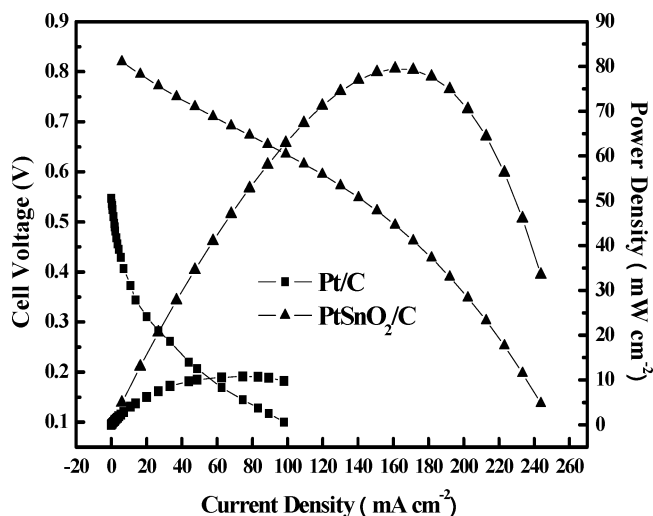


**Figure 10.** Comparison of the performance of ethanol fuel cells adopting Pt/C (commercial) and PtSnO<sub>2</sub>/C as anode electrocatalysts: operation temperature, 90 °C; ethanol concentration, 1 mol L<sup>-1</sup>; flow rate, 1 mL min<sup>-1</sup>; oxygen pressure, 0.2 MPa; noble metal loading in anode, 1.5 mg of Pt cm<sup>-2</sup>; cathode catalyst and noble metal loading, Pt/C (commercial), 1 mg of Pt cm<sup>-2</sup>; electrode membrane, Nafion-115.

#### 4. Conclusions

SnO<sub>2</sub> nanoparticles are prepared by heating ethylene glycol solutions containing SnCl<sub>2</sub> at atmospheric pressure. The XRD result shows that the obtained lightly yellow powder is spherical SnO<sub>2</sub> nanoparticles with tetragonal crystalline structure. TEM micrographs show spherical nanoparticles, the size and size distribution of which depend on the initial experimental conditions of pH value, time, and water concentration. The particle size can be controlled from 1.2 to 12 nm with the heating time increasing from 40 to 360 min. With the water content in EG solution increasing the SnO<sub>2</sub> particles gradually agglomerate. If other factors are fixed, the SnO<sub>2</sub> particle size decreases with

the pH value increasing. On the basis of the UV/vis and FTIR results, it is believed that the SnO<sub>2</sub> particles are formed by hydrolysis of SnCl<sub>2</sub>. These nanoparticles were employed to prepare carbon-supported PtSnO<sub>2</sub> catalyst, and it exhibits surprisingly high-promoting catalytic activity for ethanol electrooxidation.

**Acknowledgment.** This work was financially supported by the Innovation Foundation of the Chinese Academy of Science (Grant No. K2003D2), the National Natural Science Foundation of China (Grant No. 20173060), and the Hi-Tech Research and Development Program of China (Grant No. 2003AA517040). The Hundred Elites Program of the Chinese Academy of Sciences (Dr. Bing Zhou) is also acknowledged.

#### References and Notes

- (1) (a) Moseley, P. T. *Solid State Gas Sensors* (Review Article). *Meas. Sci. Technol.* **1997**, *8*, 223–237. (b) Liu, C. C. Nano-Crystalline Tin Oxide Film for Chemical Sensor Development. *Abstracts from the 2nd International Symposium on Electrochemical Microsystem Technologies*, Sept 9–11, 1998, Tokyo, Japan; 1998; p 32. (c) Moseley, P. T.; Norris, J.; Williams, D. E. *Techniques and Mechanisms in Gas Sensing*; Adam Hilger: Bristol, U.K., 1991.
- (2) (a) Arico, A. S.; Creti, P.; Antonucci, P. L.; Antonucci, V. *Electrochem. Solid-State Lett.* **1998**, *1*, 66. (b) Lamy, C.; Belgsir, E. M.; Leger, J.-M. *Appl. Electrochem.* **2001**, *31*, 799. (c) Zhou, W. J.; Zhou, Z. H.; Song, S. Q.; Li, W. Z.; Sun, G. Q.; Tsiakaras, P.; Xin, Q. *Appl. Catal. B* **2003**, *46*, 273. (d) Jiang, L. H.; Sun, G. Q.; Zhou, Z. H.; Zhou, W. J.; Xin, Q. *Catal. Today* **2004**, *93–95*, 665.
- (3) Zhang, G.; Liu, M. *J. Mater. Sci.* **1999**, *34*, 3213.
- (4) Mehrotra, R. C. *J. Non-Cryst. Solids* **1990**, *121*, 1.
- (5) (a) Lim, C. B.; Oh, S. *Sens. Actuators B* **1996**, *30*, 223. (b) Hiratsuka, R. S.; Snatilli, D. V.; Silva, D. V.; Pulcinelli, S. H. *J. Non-Cryst. Solids* **1992**, *147–148*, 67.
- (6) Ribeiro, C.; Lee, E. J. H.; Giraldo, T. R.; Longo, E.; Varela, J. A.; Leite, E. R. *J. Phys. Chem. B* **2004**, *108*, 15612.
- (7) Yamamoto, O.; Sasamot, T. *J. Mater. Res.* **1992**, *7*, 2488.
- (8) (a) Pan, Z. W.; Dai, Z. R.; Wang, Z. L. *Science* **2001**, *291*, 1947. (b) Wang, Y. L.; Jiang, X. C.; Xia, Y. N. *J. Am. Chem. Soc.* **2003**, *125*, 16176. (c) Gole, J. L.; Wang, Z. L. *Nano Lett.* **2001**, *1*(8), 449–451. (d) Dai, Z. R.; Gole, J. L.; Stout, J. D.; Wang, Z. L. *J. Phys. Chem. B* **2002**, *106*, 1274. (e) Deng, H. M.; Lamelas, F. J.; Hossienlopp, J. M. *Chem. Mater.* **2003**, *15*, 2429.